Spatialized Haptic Rendering: Providing Impact Position Information in 6DOF Haptic Simulations Using Vibrations

Jean Sreng* INRIA / CEA
Anatole Lécuyer† INRIA / IRISA
Claude Andriot‡ CEA
Bruno Arnaldi§ INSA / IRISA

ABSTRACT

In this paper we introduce a "Spatialized Haptic Rendering" technique to enhance 6DOF haptic manipulation of virtual objects with impact position information using vibrations. This rendering technique uses our perceptive ability to determine the contact position by using the vibrations generated by the impact. In particular, the different vibrations generated by a beam are used to convey the impact position information. We present two experiments conducted to tune and evaluate our spatialized haptic rendering technique. The first experiment investigates the vibration parameters (amplitudes/frequencies) needed to enable an efficient discrimination of the force patterns used for spatialized haptic rendering. The second experiment is an evaluation of spatialized haptic rendering during 6DOF manipulation. Taken together, the results suggest that spatialized haptic rendering can be used to improve the haptic perception of impact position in complex 6DOF interactions.

Keywords: Haptic rendering, force-feedback, vibration, spatialization, 6DOF, contact, impact, open-loop

Index Terms: H.5.1 [Information Interfaces and Presentation]: Multimedia Information Systems—Artificial, Augmented, and Virtual Realities; H.5.2 [Information Interfaces and Presentation]: User Interfaces—Haptics I/O

1 INTRODUCTION

Haptic simulation of virtual rigid bodies is increasingly used in various areas of virtual reality. 6DOF haptic rendering provides an efficient way to perceive virtual contacts by constraining the user's motion through contact forces [15, 8, 18]. This intuitive perception of contact has been used to improve the manipulation in virtual prototyping simulations, particularly for industrial assembly/disassembly/maintenance tasks [7]. However, the complex geometries of objects involved in such simulations often lead to tangled configurations. In such cases, multiple contacts blocking the objects make the manipulation difficult to understand. In these situations, classic haptic feedback providing a sole global contact force might not be sufficient to help the user to perceive the whole contact configuration. Particularly, the position of each contact is not easy to perceive.

In this paper, we propose a method to provide contact position information directly on the haptic sensory channel by using vibration patterns generated at the instant of impact [12]. An impact on a manipulated object creates high-frequency propagating vibrations that produce different transient patterns in the hand depending on the impact location on the object. These high-frequency patterns are expected to help the user in determining the impact location [21]. Therefore, we propose a "spatialized haptic rendering technique" based on these vibrations which enable the user to perceive the 3D impact position as described in Section 3. An experiment is presented in section 4 to determine a set of vibration parameters to provide an optimal rendering, *i.e.* allowing an efficient discrimination of directions among the vibrations. A preliminary evaluation of spatialized haptic rendering in virtual environment is then presented in section 5, followed by concluding remarks in section 6.

*e-mail:jean.sreng@inria.fr
†e-mail:anatole.lecuyer@irisa.fr
‡e-mail:claude.andriot@cea.fr
§e-mail:bruno.arnaldi@irisa.fr

2 RELATED WORK

Haptic rendering of simulated contacts between objects offers an intuitive way to perceive the virtual interaction. Contact forces delivered through haptic rendering, constraining the user's motion according to the virtual geometries provide essential information about the collisions. While these forces constitute an important feature of the perception of contact, some other contact mechanical properties can also be haptically perceived such as the materials of interacting objects. For instance, Klatzky and Lederman showed that surface properties such as the roughness of interacting objects can be perceived through vibratory motions during surface exploration [10]. This perceptive capability was first employed to improve the perception of contact in teleoperation contexts [11]. Furthermore, some material properties can be perceived by the high-frequency vibration caused by the sole impact between objects. Okamura *et al.* demonstrated the ability of participants to discriminate materials using these high-frequency impact vibrations [16]. They showed that combinations of vibration parameters such as amplitude slope, frequency and decay rate can enable participants to perceive different materials between rubber, wood or metal [17].

Multiple haptic rendering techniques based on this vibratory property of materials have been proposed to enhance the realism of the interaction such as texture rendering [19] or open-loop haptic [12]. In the same way, these vibrational transients can be used to convey impact location information. In a previous study, we proposed the use of the vibrations generated by different impact locations on a cantilever beam [21]. Our results suggested that participants were able to associate an impact location with a vibration pattern. Yao and Hayward investigated the perception of the length of a virtual hand-help tube through the vibrations generated by a virtual stone rolling inside the tube [24]. Their results suggested that the different vibratory cues enabled the participants to give an estimate of the length of the tube. Wang and Srinivasan studied the perception of contact distances through probe exploration [23]. They showed that participants were able to perceive this information by using either probe orientations (during unrestrained exploration) or torques (when exploration is not possible).

Tactile mappings were also used to display the contact location information by applying tactile stimulations on different positions of the hand [14]. Debus *et al.* showed that such mapping can allow the user to apply lower forces during manipulation [4]. Similarly, visual techniques have been proposed to provide this contact configuration by displaying the individual contact positions [13, 22]. Locally spatialized audio rendering of contact sounds has also been proposed [25] to improve the perception of contact position using the human ability to perceive the positions of different sound sources.

3 Spatialized Haptic Rendering: The use of vibration patterns to convey impact position information

3.1 Presentation of the vibration model

In this paper, we propose a Spatialized Haptic Rendering approach to convey 3D impact position using vibrations in addition to the classic 6DOF haptic rendering. An impact on a manipulated object creates high-frequency propagating vibrations that produce different transient patterns in the hand depending on the impact location on the object. These high-frequency patterns are expected to help the user in determining the impact location [21].

We propose to use a virtual vibrating beam metaphor held by the edge at the manipulation point. This virtual beam is vibrating according to the impact force $\mathbf{f}_\mathrm{i}$ located at the point $\mathbf{p}$. The resulting vibrations sensed in the hand depend on the position and orientation of the impact force applied on this virtual beam.

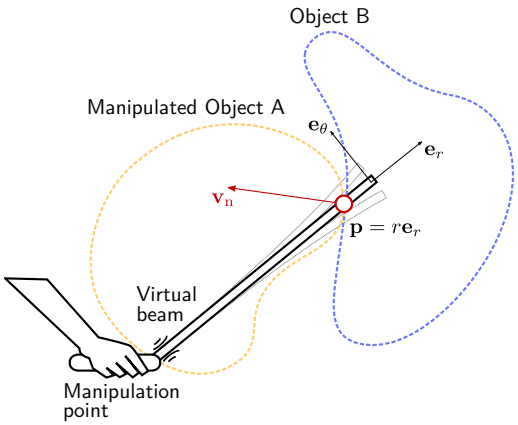

Figure 1: Description of impact and virtual beam metaphor (the handle of the haptic device is attached to Object A at the manipulation point).

This virtual beam model is similar to the 1DOF case of our previous experimental study proposed in [21] (See Figure 2). This study considered the vibrations pattern generated by the rapid deformation of a cantilever beam generated by an impact.

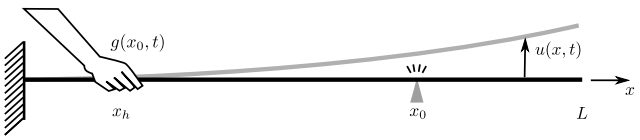

Figure 2: Cantilever vibrating beam (from [21]).

In this case, the vibration pattern sensed by the hand $g(x_0,t)$ corresponds to the displacement of the beam $u(x_h,t)$ resulting from the impact located at x_0. An evaluation was conducted to assess the ability to associate an impact position x_0 with a perceived vibration $g(x_0,t)$ using different deformation models: a physical Euler-Bernouilli model (Equ. 1) and several simplified models based on exponentially damped sinusoids (Equ. 2 for instance) :

$$g(x_0,t) = \sum_n A_n(x_0) e^{-dt} sin(\omega_n t + \phi_n) \quad (1)$$

$$g(x_0,t) = e^{-dt} sin(cd^{(L-x_0)}t) \quad (2)$$

where A_n are amplitudes of the different vibrating modes of the Euler-Bernouilli beam and c, d are chosen for a good perception of frequencies. Our previous results suggested that the participants were able to perceive the impact position, with better performances for simplified models. We proposed the model described by the Equation 2 as a "compromise between realism and performances" [21].

In our 3D approach, we consider a virtual beam located between the manipulation point and the impact point. For the sake of computation, we suggest to consider the 3D impact position $\mathbf{p}$ by using the spherical coordinate system $(\mathbf{e}_r, \mathbf{e}_\theta, \mathbf{e}_\phi)$ relative to the point $\mathbf{p}$ by considering the manipulation point as the origin so that $\mathbf{p} = r\mathbf{e}_r$ (See Figure 1). Using this description:

- The radius r providing a distance information between the hand and the impact position can be conveyed through vibration patterns based on the beam model as demonstrated in [21].
- The direction $\mathbf{e}_r$ providing the orientation of the impact with respect to the hand can be conveyed by the vibration direction. This direction information completes the spatial information of distance presented in [21].

To compute the final vibration torque, we first consider the impact force $\mathbf{f}_\mathrm{i}$ located at position $\mathbf{p}$ as being proportional to the normal impact velocity [20]:

$$\mathbf{f}_\mathrm{i} = b\,\mathbf{v}_\mathrm{n} \quad (3)$$

So that the resulting wrench $\mathbf{W}$ sensed in the hand is proportional to:

$$\mathbf{W}_\mathrm{s} = \begin{pmatrix} \tau_\mathrm{r} \\ \mathbf{f}_\mathrm{r} \end{pmatrix} = \begin{pmatrix} \mathbf{p} \wedge \mathbf{f}_\mathrm{i} \\ \mathbf{f}_\mathrm{i} \end{pmatrix} \quad (4)$$

If the 1DOF vibration model is described by $g(x,t) \in \mathbb{R}$ where x represents the distance from the hand to the impact point and t the time, we can formulate a 3DOF vibration model using the resulting wrench $\mathbf{W}_\mathrm{s}$:

$$\mathrm{W}(\mathbf{p},t) = g(|\mathbf{p}|,t)\mathbf{W}_\mathrm{s} \quad (5)$$

In particular, we can simply express the vibration torque τ as:

$$\tau(r,t) = h(r,t)\,\mathbf{e}_r \wedge \mathbf{v}_\mathrm{n} \quad (6)$$

where $h(r,t) = rb \cdot g(r,t)$ is a 1DOF generalized vibration model.

The impact distance r can thus be determined from the vibration pattern $h(r,t)$ and the impact direction $\mathbf{e}_r$ from the vibration direction $\mathbf{e}_r \wedge \mathbf{v}_\mathrm{n}$.

3.2 Manipulation point and circle of confusion

This vibration model has the main benefit to be intuitive as the torque delivered is oriented according to the impact velocity. However, even if it provides 3DOF information about the contact position (1DOF from the vibration pattern $h(r,t)$ and 2DOF from the orientation of $\mathbf{e}_r$), the exact position $\mathbf{p} = r\mathbf{e}_r$ cannot be directly deduced. Indeed, different impact positions can generate the same ambiguous vibration torque (See Figure 3). From the direction of the vibration torque τ we can only infer that $\mathbf{e}_r \perp \tau$ which means that $\mathbf{e}_r$ is on the plane perpendicular to τ. The distance information r provided by the vibration pattern $h(r,t)$ refines the position of $\mathbf{p}$ inside a "circle of confusion" defined by $\{\mathbf{x} = r\mathbf{e}_r,\ \mathbf{x} \perp \tau\}$.

Thus, the choice of the manipulation point is important to avoid similar vibratory renderings on the circle of confusion. In particular, if the manipulated part presents symmetries, the manipulation point should not be placed on the symmetry axis to avoid ambiguous situations. Two different configurations are shown in Figure 4. In the left configuration, the manipulation point and the associated circle of confusion generate the same torque for every contact point

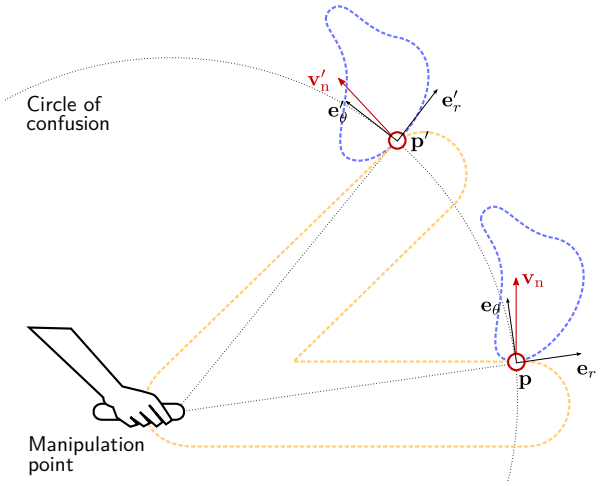

Figure 3: Circle of confusion. The two impact points $\mathbf{p}$ and $\mathbf{p}'$ generate the same vibration torque $\tau(r,t)$.

displayed. In the right configuration, only two contact points are on the circle of confusion. Moreover, in this case, the torques generated by the two contact points are oriented in opposite directions, thus resolving the ambiguity entirely.

We can notice that this ambiguity in determining the impact position is closely related to the ambiguity in perceiving the contact position solely from force and torque values.

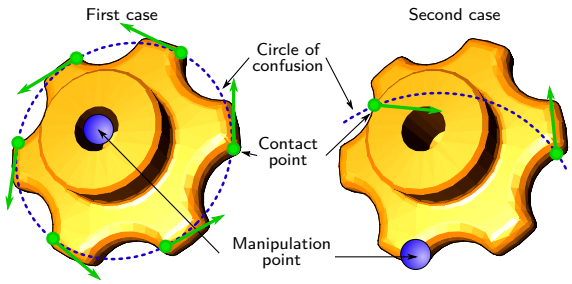

Figure 4: Two different configurations of manipulation: The manipulation point on the left is more likely to produce ambiguous vibratory renderings than the right one.

3.3 Preliminary conclusion

As a preliminary conclusion, we proposed a spatialized haptic rendering based on 3DOF vibrations of a virtual vibrating beam. This model provides an intuitive way to convey the impact position information using superimposed open-loop 3DOF vibrations. If $\Gamma(t)$ represents the total torque rendered by the haptic device, we have:

$$\Gamma(t) = \Gamma_{\text{cl}}(t) + \tau(t) \tag{7}$$

where $\Gamma_{\text{cl}}(t)$ represents the classic closed-loop torque, constraining the movement according to the contact, and $\tau(t)$ the superimposed vibration torque of spatialized haptic rendering. This torque is determined using Equation 6. In the next section, we propose to investigate parameters required to provide an optimal perception of the vibration direction.

4 Experiment 1: Determining optimal vibration parameters for spatialized haptic rendering.

4.1 Objectives

In this section, we present an experiment meant to identify the optimal parameters of our model that enable an efficient discrimination of the different vibration directions.

We propose to evaluate the perceptive ability to discriminate between different vibration directions with an exponentially damped vibration pattern, following the models described by Equation 2. In particular, we propose to determine the influence of two parameters, frequency (f) and amplitude (a):

$$h(t) = a\sin(2\pi ft)e^{-dt} \tag{8}$$

We tested this discrimination ability among the three main torque directions $\mathbf{e}_r, \mathbf{e}_\theta$ and $\mathbf{e}_\phi$. This experiment, investigating the ability to discriminate different impact directions using vibrations completes the study of [21] which was previously focused on the capacity to perceive impact distances.

4.2 Participants

10 male participants aged between 22 and 27 (mean 24.4) year volunteered for the experiment. One of them was left-handed. All participants had no perceptive disabilities and were naive about the purpose of the experiment.

4.3 Experimental apparatus

We used a Haption Virtuose6D™, an industrial device commonly used in virtual prototyping setups. The handle was constrained to a constant horizontal position. The participants were instructed to grasp the handle with their dominant hand with the grip illustrated in Figure 5. Their seat was adjusted so that their fore-arm was horizontal, making the grip comfortable. The haptic device and their fore-arm were hidden. They could only see a simple figure (See Figure 6) of the three possible vibration directions. The vibrations were only applied using the last three torque axes of the Virtuose6D™ corresponding to these three vibration directions to avoid the bandwidth loss due to the mechanical system. The haptic refresh rate was 1 kHz.

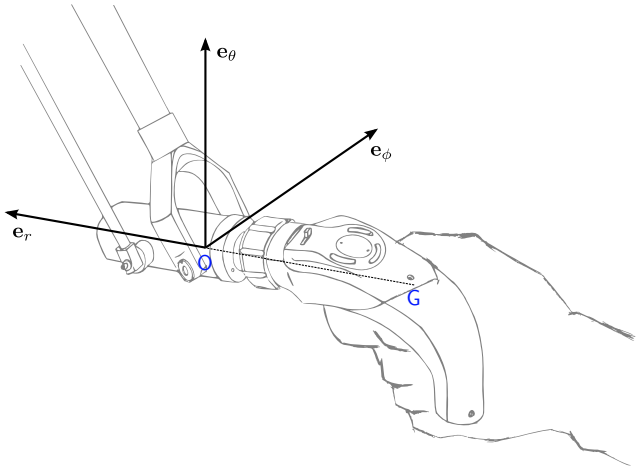

Figure 5: The three directions of torque vibration around $\mathbf{e}_r, \mathbf{e}_\theta$ and $\mathbf{e}_\phi$.

4.4 Vibration conditions

The vibration torques were applied at the mechanical rotation point O of the Virtuose6D™ (see Figure 5) around the three axes $\mathbf{e}_r, \mathbf{e}_\theta$

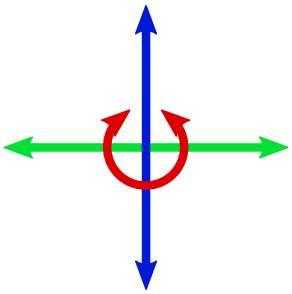

Figure 6: The figure presented to the participants: $\mathbf{e}_r$ (red arc arrow), $\mathbf{e}_\theta$ (green horizontal arrow) and $\mathbf{e}_\phi$ (blue vertical arrow).

and $\mathbf{e}_\phi$ with $\mathbf{e}_r$ being horizontal, aligned with the fore-arm. We tested the perceptive discrimination between the three axes by changing two vibration parameters:

- 4 vibration amplitudes a, respectively $a_1 = 0.02$ rad, $a_2 = 0.015$ rad, $a_3 = 0.01$ rad, $a_4 = 0.005$ rad around the axes $\mathbf{e}_\theta$ and $\mathbf{e}_\phi$ and scaled by a factor 4 around the axis $\mathbf{e}_r$ to match the lever arm difference with this axis so that the displacement amplitude of the point G (see Figure 5) is about respectively 2.4, 1.8, 1.2, 0.6 millimeters.
- 4 vibration frequencies f, respectively $f_1 = 12$ Hz, $f_2 = 18$ Hz, $f_3 = 27$ Hz, $f_4 = 40$ Hz.

The damping d was set to 5 s^{-1}. The vibration torques tested were:

$$\tau(t) = a_i \sin(\omega_j t) e^{-t} \mathbf{e}_k \quad \text{with} \quad i,j \in [\![1,4]\!], k \in \{r,\theta,\phi\} \qquad (9)$$

4.5 Procedure

The participants passively sensed the vibrations through their dominant hand. For each trial, they had to perform a three-alternative forced choice (3AFC) on the perceived direction among $\mathbf{e}_r, \mathbf{e}_\theta$ and $\mathbf{e}_\phi$. They were asked to determine, using the Figure 6, on which axis they perceived the vibration. They entered their choice using three accordingly colored buttons. The next trial started several seconds after the validation. No indication was provided about the correctness of their choice. The participants were instructed to maintain a constant grip during the whole experiment.

All the $4 \times 4 = 16$ amplitude/frequency pairs were tested on the 3 axes in a random order, totalizing for each block $16 \times 3 = 48$ trials. All participants tested 15 repetitions of amplitude/frequency/axis condition in 15 random blocks for a total of $48 \times 15 = 720$ trials. The duration of one trial was approximatively 2–3 sec. After the trials they were debriefed and asked about their strategy and were free to give any additional comments. The total time of the experiment (including preliminary explanations and debriefing) did not exceed 40 minutes.

4.6 Results

The proportion of correct responses (when the participant correctly perceived the vibration axis) was evaluated for each participant for the 4 amplitudes $\times$ 4 frequencies $\times$ 3 axes = 48 conditions (See Tables 1,2,3). A random choice between the three directions corresponds to a chance proportion of $1/3$ (a participant unable to perceive a vibration axis is expected to provide random responses).

The boxplots of the overall results gathered for the different amplitudes, frequencies and axes are respectively provided in Figures 7, 8, 9.

Performances reached almost 100% of correct responses with amplitude a_1 and frequency f_1 on the three axes. The two highest amplitudes a_1, a_2 and lowest frequencies f_1, f_2 achieved more

m	a_1	a_2	a_3	a_4
f_1	0.96	0.94	0.94	0.87
f_2	0.93	0.86	0.85	0.76
f_3	0.85	0.90	0.85	0.71
f_4	0.84	0.86	0.75	0.74

σ	a_1	a_2	a_3	a_4
f_1	0.04	0.07	0.06	0.18
f_2	0.08	0.12	0.13	0.19
f_3	0.15	0.10	0.13	0.19
f_4	0.16	0.12	0.16	0.17

Table 1: Mean (m) and standard deviation (σ) of correct responses for each amplitude/frequency (a_i, f_j) pair for axis $\mathbf{e}_r$. $a_1 = 0.02$ rad, $a_2 = 0.015$ rad, $a_3 = 0.01$ rad, $a_4 = 0.005$ rad and $f_1 = 12$ Hz, $f_2 = 18$ Hz, $f_3 = 27$ Hz, $f_4 = 40$ Hz.

m	a_1	a_2	a_3	a_4
f_1	0.99	0.95	0.88	0.79
f_2	0.93	0.95	0.92	0.82
f_3	0.91	0.92	0.80	0.66
f_4	0.80	0.66	0.52	0.47

σ	a_1	a_2	a_3	a_4
f_1	0.02	0.05	0.11	0.19
f_2	0.06	0.05	0.08	0.15
f_3	0.09	0.13	0.13	0.19
f_4	0.20	0.25	0.19	0.26

Table 2: Mean (m) and standard deviation (σ) of correct responses for each amplitude/frequency (a_i, f_j) pair for axis $\mathbf{e}_\theta$. $a_1 = 0.02$ rad, $a_2 = 0.015$ rad, $a_3 = 0.01$ rad, $a_4 = 0.005$ rad and $f_1 = 12$ Hz, $f_2 = 18$ Hz, $f_3 = 27$ Hz, $f_4 = 40$ Hz.

m	a_1	a_2	a_3	a_4
f_1	0.97	0.95	0.91	0.73
f_2	0.96	0.98	0.86	0.61
f_3	0.96	0.91	0.78	0.74
f_4	0.92	0.91	0.74	0.60

σ	a_1	a_2	a_3	a_4
f_1	0.04	0.05	0.10	0.17
f_2	0.03	0.04	0.11	0.19
f_3	0.07	0.12	0.22	0.18
f_4	0.09	0.12	0.24	0.24

Table 3: Mean (m) and standard deviation (σ) of correct responses for each amplitude/frequency (a_i, f_j) pair for axis $\mathbf{e}_\phi$. $a_1 = 0.02$ rad, $a_2 = 0.015$ rad, $a_3 = 0.01$ rad, $a_4 = 0.005$ rad and $f_1 = 12$ Hz, $f_2 = 18$ Hz, $f_3 = 27$ Hz, $f_4 = 40$ Hz.

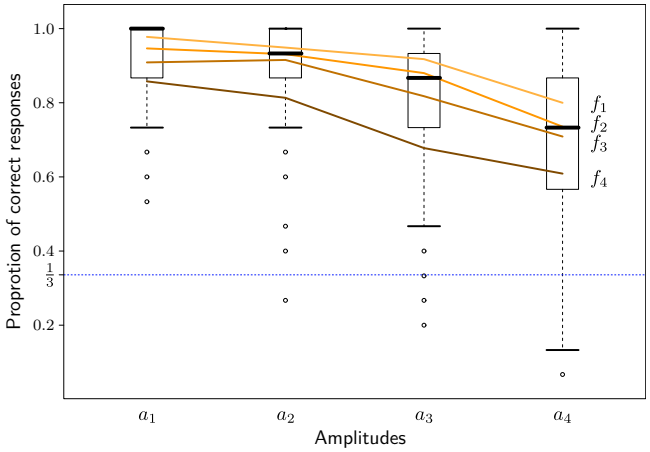

Figure 7: Proportion of correct responses for each amplitude level. Proportion means for each frequency level are superimposed.

than 90% correct responses on axes $\mathbf{e}_\theta$ and $\mathbf{e}_\phi$. The dispersion of the proportion of correct responses is very low when this proportion is high and increases for lower scores. We could notice that among all the participants, one participant achieved a quasi-perfect performance among the whole amplitude and frequency range on the three axes.

A three-way within subject design ANOVA was performed on

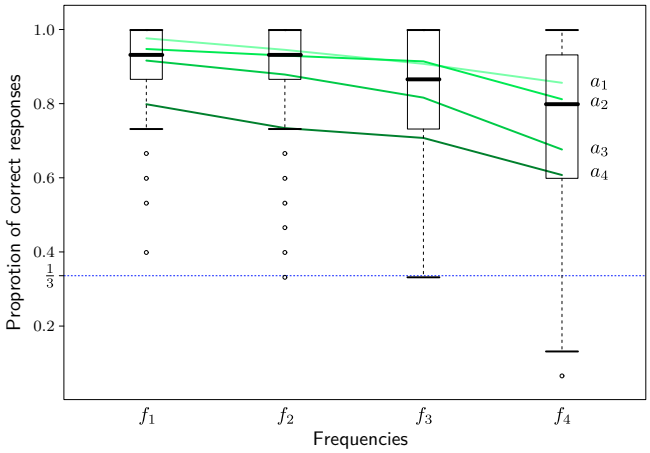

Figure 8: Proportion of correct responses for each frequency level. Proportion means for each amplitude level are superimposed.

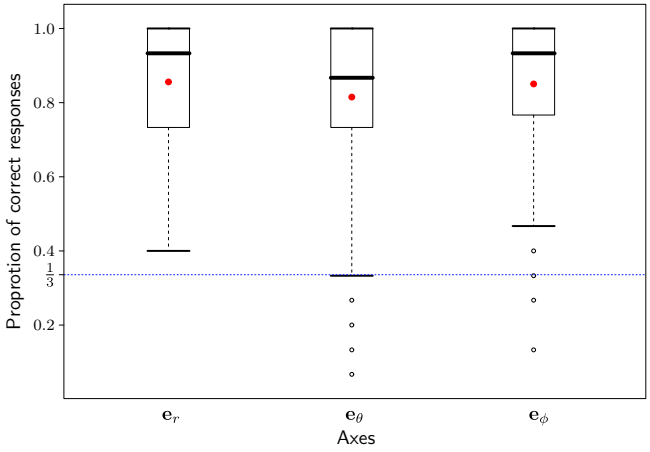

Figure 9: Proportion of correct responses for each axis. Means are indicated by red dots.

the amplitude, frequency and axis factors. The summary of the analysis is presented in Table 4.

Factor	df	F value	p	Sig. level
Amp	3	72.87	$< 10^{-6}$	***
Freq	3	43.85	$< 10^{-6}$	***
Axis	2	5.29	0.0053	**
Amp×Freq	9	1.40	0.1847	
Amp×Axis	6	3.69	0.0013	**
Freq×Axis	6	9.32	$< 10^{-6}$	***
Amp×Freq×Axis	18	1.38	0.1354	

Table 4: Three-way within subject design ANOVA. Significance levels: (*) $p < 0.05$, (**) $p < 0.01$, (***) $p < 0.001$

This analysis finds significant differences between the means of proportion of correct responses among different amplitudes, frequencies and axes. There seems to be no interaction effect between amplitude and frequency factors on the performances. However the variation of performances for different amplitudes and frequencies seems to depend on the axis. The paired t-tests between the axes $\mathbf{e}_\theta$,$\mathbf{e}_\phi$ ($t(159) = -2.35$, $p < 0.02$) and $\mathbf{e}_\theta$,$\mathbf{e}_r$ ($t(159) = -2.65$, $p < 0.009$) were significant, and not significant between the axes $\mathbf{e}_r$,$\mathbf{e}_\phi$ ($t(159) = -0.37$, $p = 0.7$).

4.7 Discussion

Our results indicate that the participants were able to efficiently perceive the different directions of vibration along the three axes $\mathbf{e}_r, \mathbf{e}_\theta$ and $\mathbf{e}_\phi$. The best discrimination performance was achieved for high amplitude values and low frequency values.

The amplitude range of 0.005 rad to 0.02 rad and frequency range of 12 Hz to 40 Hz enable good perceptive performances, *i.e.* more than 80% or correct direction perceived on the three axes (Figure 9). These ranges seem thus to constitute a first set of efficient vibration parameters allowing a good direction discrimination.

Several participants however reported during debriefing after the experiment that too high amplitudes (a_1) made their perception more difficult, particularly on axes $\mathbf{e}_\theta$ and $\mathbf{e}_\phi$, in particular for high frequencies. The perception of vibration direction seems to be performed through the relative contributions of the tactile perception in the hand and the kinesthetic perception in the whole arm. High vibration amplitudes delivered to the hand may generate some "parasite movements" depending on the grip of the user on the whole hand–fore-arm–arm chain. These parasite movements may impair the kinesthetic perception of vibration direction. Low frequencies seem to enable a better perception of vibration directions, suggesting the relative importance of kinesthetic perception since the tactile detection threshold in the hand is decreasing in the considered frequency range [2] whereas the kinesthetic perception bandwidth does not exceed 20–30 Hz [3]. Tactile perception seems also to be important, particularly for small amplitudes and high frequencies as several participants commented that they relied on tactile perception on the palm, particularly to distinguish axis $\mathbf{e}_r$ in such cases.

There seems to be no interaction between the amplitude and frequency factors on the perception of vibration direction in the range of values we tested. This appears to be consistent with previous studies on the perception of movement showing that velocity does not influence the direction detection threshold for simple movements on the shoulder and elbow above 5°/s [5].The influence of axis on the performance can be simply described by the assymmetry of both the vibration stimulus applied on the hand, and the perceptive system of the hand–fore-arm–arm chain.

When asked about their perception strategies, most of the participants reported that they did not use a particular strategy but relied on the intuitive perception of direction.

These results show that vibration discrimination is possible among the three axes $\mathbf{e}_r, \mathbf{e}_\theta$ and $\mathbf{e}_\phi$ for the amplitude and frequency range tested. This perception is improved for high amplitudes and low frequencies. However, further work could determine more precisely the perceptive characteristics associated with the perception of vibration direction such as JNDs (Just Noticeable Differences) and PSEs (Point of Subjective Equality). As a comparison, we can notice that the perception resolution of limb movement is between 0.8–7° [9] and the force direction threshold has been found around 25° [1].

In the next section we present an implementation of spatialized haptic rendering in a virtual prototyping application using amplitude and frequency values located in the range of values identified in this first experiment.

5 Experiment 2: Preliminary Evaluation of Spatialized Haptic Rendering

We implemented our spatialized haptic rendering technique in an existing haptic setup dedicated to virtual prototyping. We con-

ducted a preliminary evaluation to assess the potential benefit of this technique in a real case.

5.1 Participants

11 participants (8 males, 3 females) aged between 25 and 43 (mean 31) years, volunteered for the experiment. All participants had no perceptive disabilities and were naive about the purpose of the experiment. Two of them where altough familiar with haptic rendering devices.

5.2 Procedure

Participants were asked to test two different haptic rendering techniques successively, without any additional information about the techniques. To do so, they were instructed to simply freely interact with two complex objects and feel the different sensations related to the contacts (See Figure 10 and 11). The haptic refresh rate was 1 kHz.

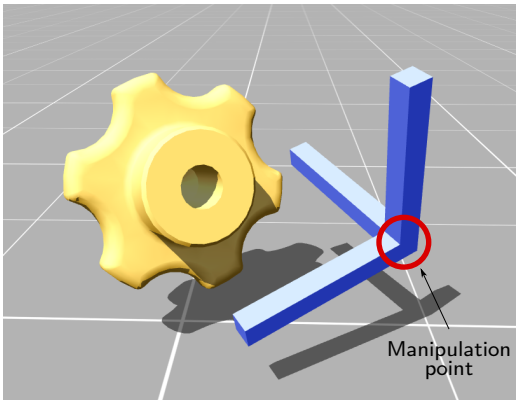

Figure 10: Haptic use-case. The participants were instructed to manipulate the blue part and feel the contacts with the yellow part.

Figure 11: Experimental setup.

We presented successively, in a balanced order, the classic haptic feedback (such as in [15, 8, 18] for instance) delivered by the virtual prototyping simulation without (condition A) and with (condition B) our superimposed spatialized haptic rendering. We adopted the following parameters for the vibration model:

$$h(x,t) = a\left(\frac{x}{L}\right)\sin\left(2\pi f\left(\frac{x}{L}\right)t\right)e^{-5t} \tag{10}$$

with

$$\begin{cases} a(r) &= a_{\max}r + a_{\min}(1-r) \\ f(r) &= f_{\min}r + f_{\max}(1-r) \end{cases} \tag{11}$$

were L represents the maximum length of the object from the manipulation point. The amplitude $(a_{\min}, a_{\max})$ and frequency $(f_{\min}, f_{\max})$ values were chosen inside the ranges tested in section 4 that were found to globally allow a good perception of vibration directions. Besides, these values provide a dynamic range large enough to enable a good discrimination between different impact distances:

$$a_{\min}, a_{\max} = (0.005, 0.02) \tag{12}$$
$$f_{\min}, f_{\max} = (15, 40) \tag{13}$$

Last, participants were presented a questionnaire:

- They were first asked if they felt any difference between the two conditions.
- For each condition, they were asked to rate from 1 to 6 (1 being the worse and 6 the better) the three following criteria: impact realism, feeling of impact position, and overall comfort of manipulation.
- Finally they were asked which one (from the two rendering techniques) they would select in a similar virtual prototyping environment.

5.3 Results

Among the 11 participants, 10 perceived the difference between the two haptic rendering techniques. The rating results collected with these 10 participants are presented in Table 5 and Figure 12. The Mann-Whitney-Wilcoxon (MWW) test on the ratings about the perception of impact position was significant ($V = 6.5$, $p = 0.023 < 0.05$). However, the MWW test on impact realism ($V = 6.5$, $p = 0.12$) and comfort ($V = 6.5$, $p = 0.8$) were not significant.

70% of the participants reported that they would use the spatialized haptic rendering technique in a similar virtual prototyping environment.

Feedback type	Impact realism	Impact position	Comfort
Without vib.	3.3 (1.25)	3.3 (1.5)	4 (1.15)
With vib.	4.3 (1.34)	4.6 (1.17)	3.8 (1.7)

Table 5: Mean values and standard deviation m (σ) of subjective ratings about the impact realism, the feeling of impact position and the overall comfort with and without spatialized haptic rendering.

5.4 Discussion

This preliminary evaluation suggests that spatialized haptic rendering improves the sensation of impact position in 6DOF haptic manipulations. Moreover, several participants spontaneously reported during the experiment that the rendering technique B (with vibrations) provided them with a "spatial feeling" of the contact enabling them to determine the contact position in visual ambiguous situation.

Most participants pointed out that they perceived different materials between the conditions. They described the material as "harder" or "crisper" using the rendering technique B (with vibrations) which correlates with the studies on open-loop haptics [17, 12]. Several participants who noticed explicitly the superimposed vibrations reported that they perceived a vibrating metal or plastic material in such condition. However, two of them reported that they perceived these vibrations as being caused by an unstable

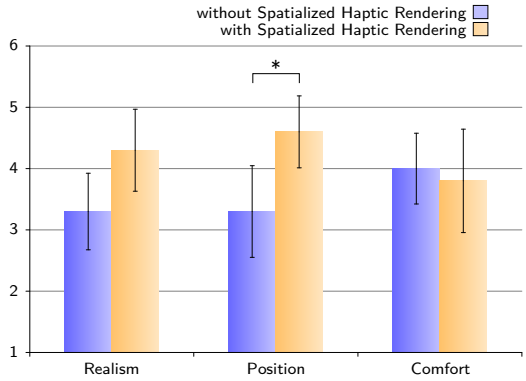

Figure 12: Mean and standard deviation of subjective ratings about the impact realism, the feeling of impact position and the overall comfort. Statistically significant differences are shown by (*).

simulation (they consequently preferred the condition A in the last question). These two participants were actually familiar with haptic rendering algorithms. For them, vibrations are always associated to an instable, potentially harmful, control behavior.

As a concluding remark, many participants reported that they enjoyed the manipulation using haptic rendering technique B (with vibrations) as being more realistic, and providing some contact sensations that they did not feel using the rendering technique A (without vibrations).

6 Conclusion

In this paper we proposed a spatialized haptic rendering technique to provide 3D impact location information in 6DOF manipulations using vibration patterns. These vibration patterns are based on a 3DOF vibrating beam model held by one edge: different vibrations resulting from the rapid displacement of the beam are generated by multiple impact positions. These different vibrations, sensed with the hand, can convey the impact position information to the user. Then, we presented an experiment to determine the vibration parameters (amplitudes and frequencies) enabling an efficient discrimination of vibrations. We finally conducted a preliminary evaluation in a real haptic manipulation setup dedicated to virtual prototyping. The results suggest that spatialized haptic rendering enables a better perception of impact position and higher feeling of realism.

Future work will first consist in conducting a quantitative evaluation to provide a more precise analysis of the effect of this technique in a virtual prototyping context. We would also like to investigate more deeply the perceptive characteristics (JND/PSE) associated with the contact position information and the influence of multiple vibratory models and parameters [6].

References

[1] F. Barbagli, J. K. Salisbury, C. Ho, C. Spence, and H. Z. Tan. Haptic discrimination of force direction and the influence of visual information. *ACM Transactions on Applied Perception*, 3(2):125–135, 2006.

[2] S. J. Bolanowsky Jr., G. A. Gescheider, R. T. Verrillo, and C. M. Checkosky. Four channels mediate the mechanical aspects of touch. *Journal of the Acoustical Society of America*, 84(5):1680–1694, 1988.

[3] T. L. Brooks. Telerobotics response requirements. In *Proceedings of IEEE International Conference on Systems, Man, and Cybernetics*, pages 113–120, 1990.

[4] T. Debus, T.-J. Jang, P. Dupont, and R. D. Howe. Multi-channel vibrotactile display for teleoperated assembly. In *Proceedings of IEEE International Conference on Robotics and Automation*, pages 592–597, 2002.

[5] L. A. Hall and D. I. McCloskey. Detections of movements imposed on finger, elbow and shoulder joints. *The journal of physiology*, 335:519–533, 1983.

[6] A. Israr, S. Choi, and H. Z. Tan. Detection threshold and mechanical impedance of the hand in a pen-hold posture. In *Proceedings of International Conference on Intelligent Robots and Systems*, pages 472–477, 2006.

[7] S. Jayaram, U. Jayaram, Y. Wang, H. Tirumali, K. W. Lyons, and P. Hart. Vade: A virtual assembly design environment. *Virtual Reality*, 19(6):44–50, 1999.

[8] D. E. Johnson and P. Willemsen. Six degree-of-freedom haptic rendering of complex polygonal models. In *Proceedings of 11th Symposium on Haptic Interfaces for Virtual Environment and Teleoperator Systems*, 2003.

[9] L. A. Jones. Kinesthetic sensing. In *Proceedings of Workshop on Human and Machine Haptics*. MIT Press, 1997.

[10] R. L. Klatzky and S. J. Lederman. Perceiving texture through a probe. In M. L. McLaughlin, G. S. Sukhatme, and J. P. Hespanha, editors, *Touch in Virtual Environments: Haptics and the Design of Interactive Systems*, chapter 10, pages 180–193. Prentice Hall PTR, Upper Saddle River, NJ, USA, 2002.

[11] D. A. Kontarinis and R. D. Howe. Tactile display of vibratory information in teleoperation and virtual environments. *Presence*, 4(4):387–402, 1995.

[12] K. J. Kuchenbecker, J. Fiene, and G. Niemeyer. Improving contact realism through event-based haptic feedback. *IEEE Transactions on Visualization and Computer Graphics*, 12(2):219–230, 2006.

[13] A. Lécuyer, C. Mégard, J.-M. Burkhardt, T. Lim, S. Coquillart, P. Coiffet, and L. Graux. The effect of haptic, visual and auditory feedback on an insertion task on a 2-screen workbench. In *Proceedings of Immersive Projection Technology Symposium*, 2002.

[14] M. J. Massimino and T. B. Sheridan. Sensory substitution for force feedback in teleoperation. *Presence*, 2(4):344–352, 1993.

[15] W. A. McNeely, K. D. Puterbaugh, and J. J. Troy. Six degree-of-freedom haptic rendering using voxel sampling. In *Proceedings of ACM SIGGRAPH'99*, pages 401–408, 1999.

[16] A. M. Okamura, J. T. Dennerlein, and R. D. Howe. Vibration feedback models for virtual environments. In *Proceedings of International Conference on Robotics and Automation*, pages 674–679, 1998.

[17] A. M. Okamura, M. W. Hage, J. T. Dennerlein, and M. R. Cutkosky. Improving reality-based models for vibration feedback. In *Proceedings of ASME Dynamic Systems and Control Division*, pages 1117–1124, 2000.

[18] M. A. Otaduy and M. C. Lin. A modular haptic rendering algorithm for stable and transparent 6-DOF manipulation. *IEEE Transactions on Robotics*, 22(4):751–762, 2006.

[19] J. Siira and D. K. Pai. Haptic texturing - a stochastic approach. In *Proceedings of International Conference on Robotics and Automation*, pages 557–562, 1996.

[20] J. Sreng, F. Bergez, J. Legarrec, A. Lécuyer, and C. Andriot. Using an event-based approach to improve the multimodal rendering of 6DOF virtual contact. In *Proceedings of the ACM symposium on Virtual reality software and technology*, pages 165–173, 2007.

[21] J. Sreng, A. Lécuyer, and C. Andriot. Using vibration patterns to provide impact position information in haptic manipulation of virtual objects. In M. Ferre, editor, *Proceedings of Eurohaptics 2008*, volume 5024 of *Lecture Notes in Computer Science*, pages 589–598. Springer-Verlag, 2008.

[22] J. Sreng, A. Lécuyer, C. Mégard, and C. Andriot. Using visual cues of contact to improve interactive manipulation of virtual objects in industrial assembly/maintenance simulations. *IEEE Transactions on Visualization and Computer Graphics*, 12(5):1013–1020, 2006.

[23] S. Wang and M. A. Srinivasan. The role of torque in haptic perception of object location in virtual environments. In *Proceedings of 11th Symposium on Haptic Interfaces for Virtual Environment and Teleoperator Systems*, 2003.

[24] H.-Y. Yao and V. Hayward. An experiment on length perception with a virtual rolling stone. In *Proceedings of Eurohaptics*, pages 325–330, 2006.

[25] Y. Zhang, T. Fernando, H. Xiao, and A. R. L. Travis. Evaluation of auditory and visual feedback on task performance in a virtual assembly environment. *Presence*, 15(6):613–626, 2006.